Electronic Supplementary Information (ESI)

Does Li-Ion Transport Occur Rapidly in Localized High-Concentration Electrolytes?

Yoshifumi Watanabe,[a] Yosuke Ugata,[a,b] Kazuhide Ueno, [a,b] Masayoshi Watanabe, [b] Kaoru Dokko [a,b,*]

[a] *Department of Chemistry and Life Science, Yokohama National University, 79-5 Tokiwadai, Hodogaya-ku, Yokohama 240-8501, Japan*

[b] *Advanced Chemical Energy Research Center (ACERC), Institute of Advanced Sciences, Yokohama National University, 79-5 Tokiwadai, Hodogaya-ku, Yokohama 240-8501, Japan*

*CORRESPONDING AUTHOR

E-mail: dokko-kaoru-js@ynu.ac.jp (K.D.)

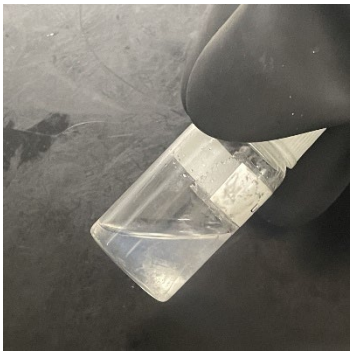

Figure S1. Photograph of a [LiFSA]/[SL]/[HFE] = 1/2.5/3 mixture after storage for several weeks at room temperature.

Table S1. Concentration of LiFSA (c), viscosity (η), ionic conductivity (σ), molar conductivity (Λ), Li^+ ion transference number (t_{Li}^{abc}), and product of σ and t_{Li}^{abc} of [LiFSA]/[SL]/[HFE] = 1/2.5/n electrolytes at 30 ºC

[LiFSA]/[SL]/[HFE] = 1/2.5/*n*	***c*** **(mol dm^{-3})**	***η*** **(mPa s)**	***σ*** **(mS cm^{-1})**	***Λ*** **(S cm^2 mol^{-1})**	t_{Li}^{abc} **(-)**	$t_{Li}^{abc} \times \sigma$ **(mS cm^{-1})**
n = 0	3.05	165.8	1.90	0.62	0.53(±0.02)	1.00(±0.04)
n = 0.5	2.49	79.0	2.07	0.83	0.43(±0.02)	0.89(±0.04)
n = 1	2.10	44.2	2.21	1.03	0.39(±0.00)	0.86(±0.01)
n = 2	1.60	20.0	2.08	1.30	0.38(±0.03)	0.79(±0.07)

Table S2. Diffusivities of Li^+ (D_{Li}), FSA^- (D_{FSA}), SL (D_{SL}), HFE (D_{HFE}), and calculated molar conductivity Λ_{NE} based on the Nernst-Einstein relation in the [LiFSA]/[SL]/[HFE] = 1/2.5/n electrolytes at 30 ºC.

[LiFSA]/[SL]/[HFE] = 1/2.5/*n*	D_{Li} **(cm^2 s^{-1})**	D_{FSA} **(cm^2 s^{-1})**	D_{SL} **(cm^2 s^{-1})**	D_{HFE} **(cm^2 s^{-1})**	Λ_{NE} **(S cm^2 mol^{-1})**
n = 0	1.37×10^{-7}	9.39×10^{-8}	8.79×10^{-8}	—	0.85
n = 0.5	1.62×10^{-7}	1.64×10^{-7}	1.63×10^{-7}	2.62×10^{-7}	1.20
n = 1	2.12×10^{-7}	2.39×10^{-7}	2.41×10^{-7}	4.46×10^{-7}	1.67
n = 2	3.45×10^{-7}	4.30×10^{-7}	4.62×10^{-7}	1.11×10^{-6}	2.86

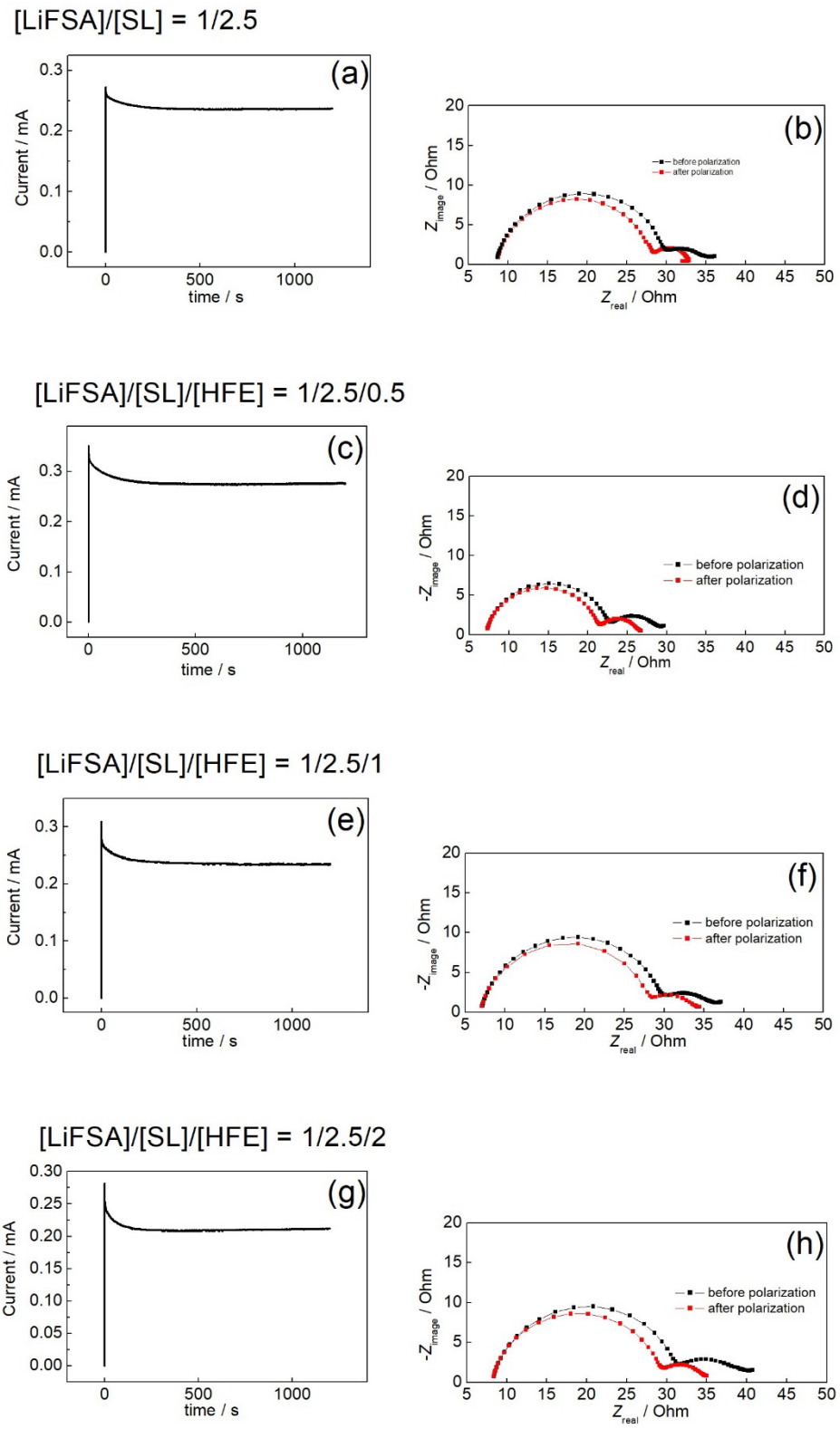

Figure S2. (a), (c), (e), (g): Chronoamperograms of Li/Li symmetric cells measured at a constant voltage, ΔV of 10 mV. (b), (d), (f), (h): Nyquist plots of cells before and after chronoamperometry with [LiFSA]/[SL]/[HFE] = 1/2.5/n (n = 0, 0.5, 1, 2) electrolytes.

Oxidative stability of the LiFSA/SL/HFE electrolytes.

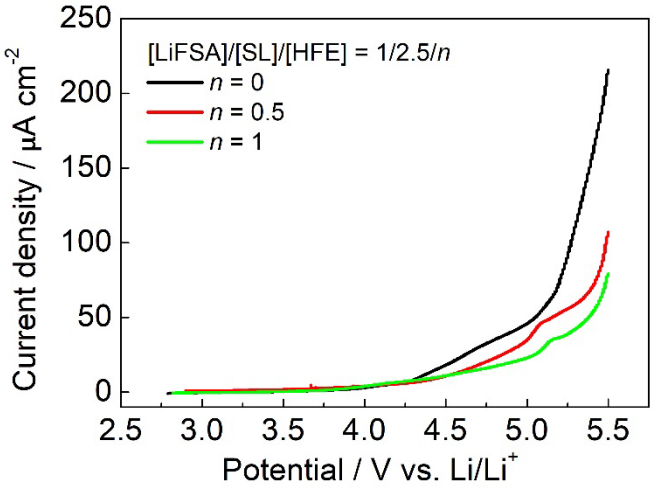

Figure S3. Linear sweep voltammograms for [LiFSA]/[SL]/[HFE] = 1/2.5/*n* electrolytes measured at a scan rate of 1 mV s^{-1} at 30 °C. Linear sweep voltammetry was performed using a two-electrode cell comprising Li metal (13-mm diameter) and Pt metal (13-mm diameter) electrodes and a GA-55 separator (13-mm diameter) wetted with electrolyte (100 μL).

Li deposition and dissolution in the LiFSA/SL/HFE electrolytes.

Li deposition and stripping on a Cu electrode was performed using 2032-type coin cells with a Li|electrolyte|Cu configuration (**Figure S4**). The cell was assembled using Li metal foil (16-mm diameter), a porous polyolefin film (Celgard 3501, 17-mm diameter) wetted with an electrolyte (100 μL), and Cu foil (16-mm in diameter). Repetitive Li deposition-stripping cycles were conducted by deposition of Li at 0.2 mA cm^{-2} for 2.5 h followed by stripping at 0.2 mA cm^{-2}. Stripping was terminated when the cell voltage reached at 2 V. The cycling tests were conducted at 30 ºC.

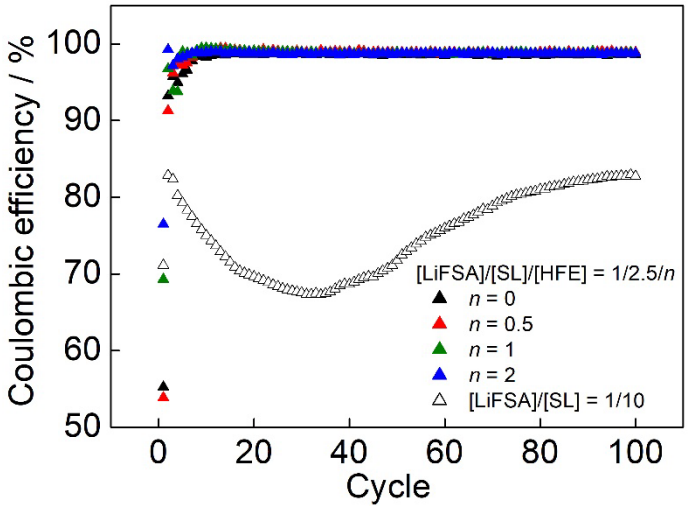

Figure S4. Coulombic efficiency of Li deposition/stripping in [LiFSA]/[SL]/[HFE] = 1/2.5/*n* and [LiFSA]/[SL] = 1/10 electrolytes at 30 °C.

Scanning electron microscopy of Li metal deposited deposited from LiFSA/SL/HFE electrolytes.

Li deposits on the Cu electrode were observed using a scanning electron microscope (SEM; SU8010, Hitachi High-Technologies). Li metal was deposited in a 2032-type coin cell with a Li|electrolyte|Cu configuration. The cell was assembled using Li metal foil (16-mm diameter), a Celgard 3501 film (17-m diameter) wetted with electrolyte (100 μL), and a Cu metal foil (16-mm diameter). Li was deposited on the Cu electrode at a current density of 0.2 mA cm^{-2} for 10 h. The cell was disassembled in an Ar-filled glove box, and the Li-on-Cu electrode was washed with dimethoxymethane (DME) to remove residual electrolyte. Samples were transferred to the SEM chamber using an Air-tight transfer vessel.

Figure S5 shows SEM images of Li metal deposited from [LiFSA]/[SL]/[HFE] = 1/2.5/*n* electrolytes. Granular Li deposits form in all electrolytes. Dendritic Li growth is hindered in these electrolytes in agreement with results reported in Ref. S1. The granular Li deposits have small surface areas compared to dendritic Li deposits, which may be effective in suppressing side reactions between Li metal and the electrolyte.

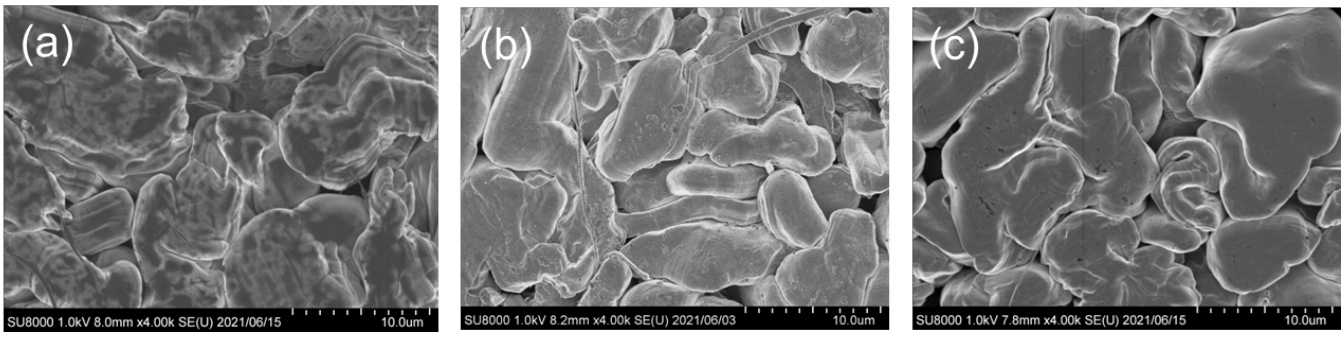

Figure S5. SEM images of Li metal deposited on the Cu electrode at a current density of 0.2mA cm^{-2} for 10 h. Electrolyte compositions: (a) [LiFSA]/[SL] = 1/2.5, (b) [LiFSA]/[SL]/[HFE] = 1/2.5/1, and (c) [LiFSA]/[SL]/[HFE] = 1/2.5/2.

X-ray photoelectron spectroscopy of Li metal deposited from LiFSA/SL/HFE electrolytes.

X-ray photoelectron spectroscopy (XPS) was conducted on Cu electrodes deposited with Li metal. 2032-type coin cells were assembled using Li metal foil (16-mm diameter), a Celgard 3501 film (17-m diameter) wetted with electrolyte (100 μL), and a Cu metal foil (16-mm diameter). Prior to XPS analysis, 20 Li deposition-stripping cycles were conducted at 0.2 mA cm^{-2} and 2.5 h for deposition and at 0.2 mA cm^{-2} for stripping. The cell was disassembled in an Ar-filled glove box, and the Li-on-Cu electrode was washed with dimethoxymethane (DME) to remove residual electrolyte. Samples were transferred to the XPS chamber using an Air-tight transfer vessel. XPS was conducted using a VersaProbe II (Ulavac-phi) spectrometer with an Al Kα X-ray source at a base pressure of 7.1×10^{-8} Pa.

Figure S6 shows XPS spectra of the Li metal deposited on the Cu electrode. The samples deposited from the [LiFSA]/[SL]/[HFE] = 1/2.5/*n* electrolytes show similar spectra regardless of the HFE content, in agreement with the results reported in Ref. S1. The peaks at 284.8 and 286.5 eV in the C 1s spectra are assigned to C–C and C–O entities, respectively, originating from the decomposition of SL. The peaks at 158–163 and 164–172 eV in the S 2p spectra are assigned to Li_2S and $–SO_x$ units, respectively, arising from the decomposition of FSA^- and SL. Peaks corresponding to SO_2 and Li_2O are observed in the O 1s spectra and are assigned to FSA^- and SL decomposition products. The peaks assignable to LiF in the F 1s and Li 1s spectra are consistent with the decomposition of FSA^- on Li metal. LiF is an electronic insulator and may function as a solid-electrolyte interphase (SEI) and suppress further reductive decomposition of the electrolyte on Li metal.

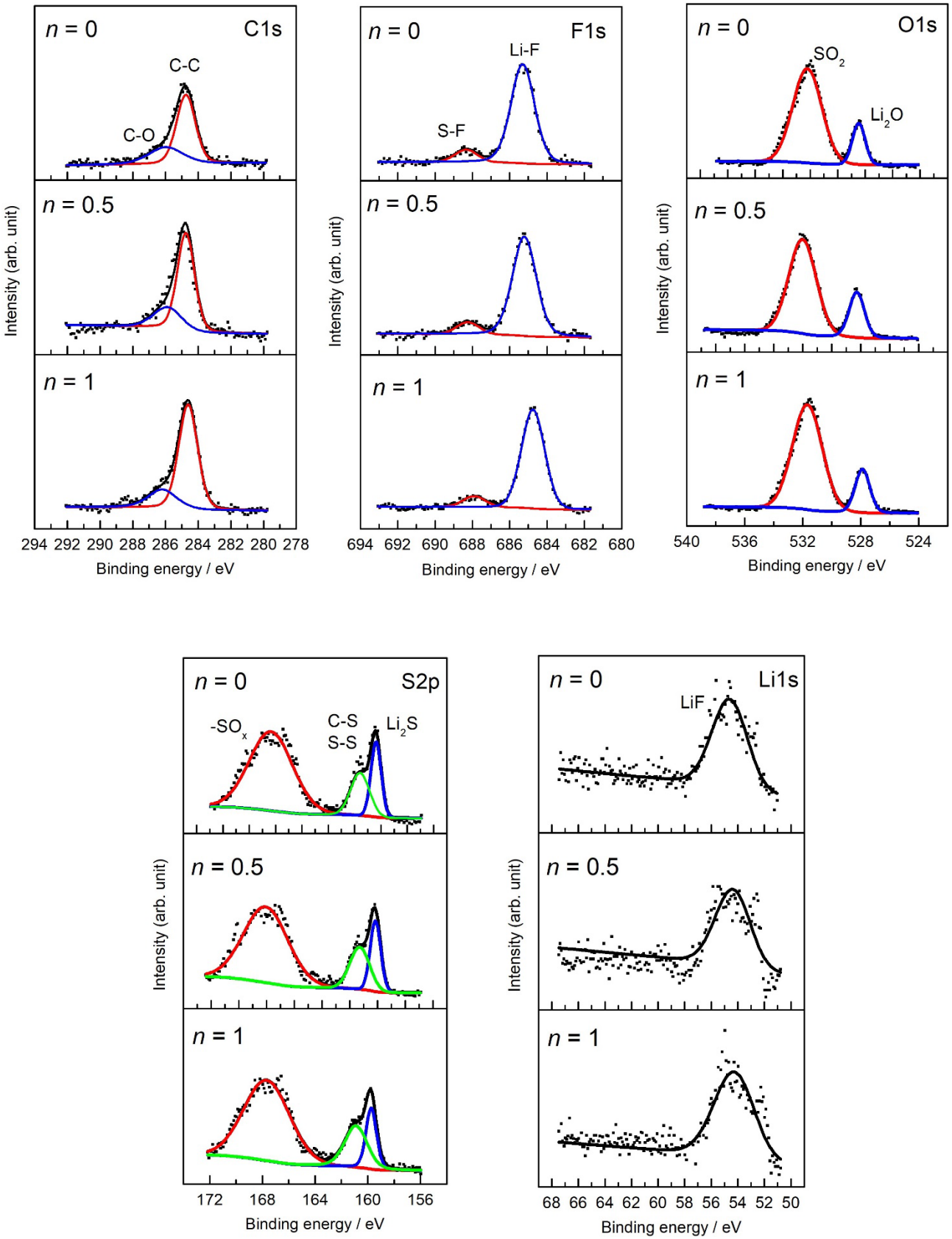

Figure S6. XPS spectra of Li deposited on Cu electrodes in the [LiFSA]/[SL]/[HFE] = 1/2.5/*n* electrolytes.

Battery tests of LiFSA/SL/HFE electrolytes.

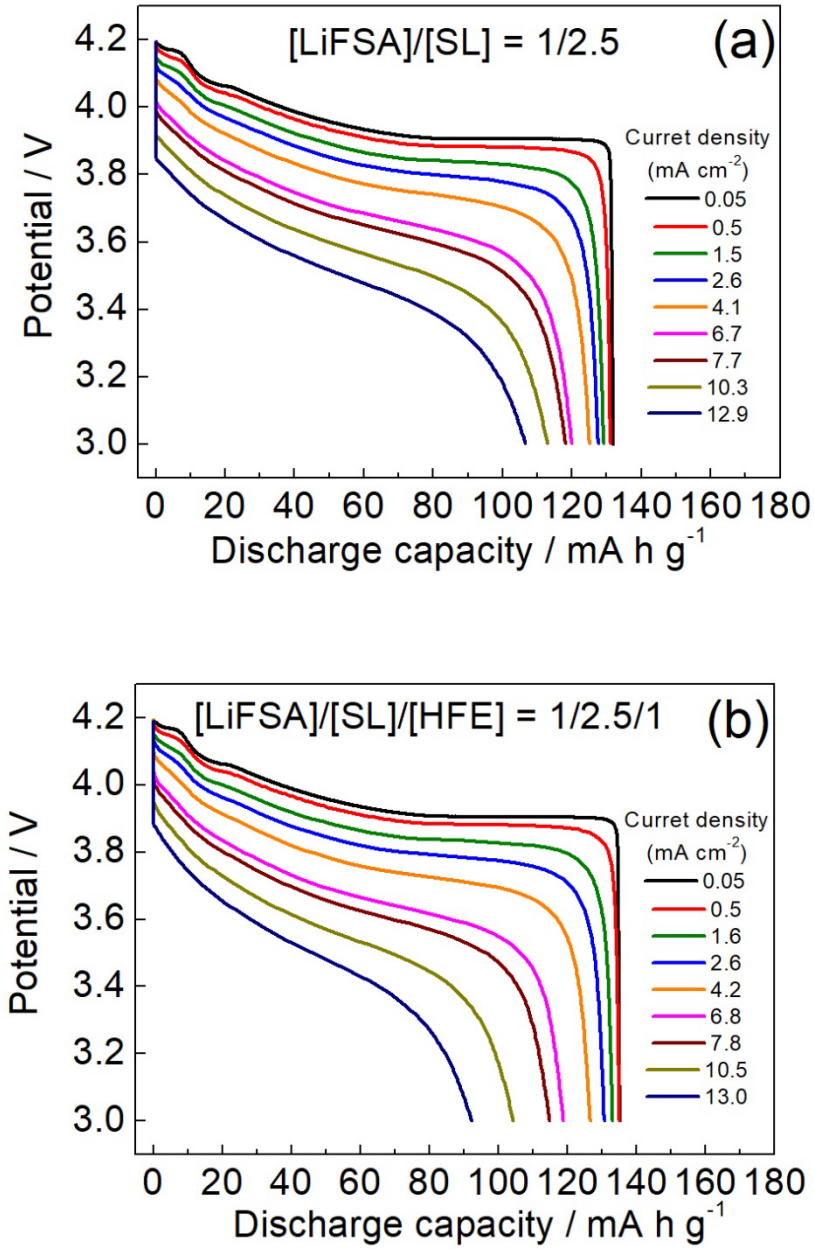

Figure S7. Discharge curves of Li/$LiCoO_2$ cells with (a) [LiFSA]/[SL] = 1/2.5 and (b) [LiFSA]/[SL]/[HFE] = 1/2.5/1 electrolytes measured at different current densities at 30 ºC. The cells were charged to 4.2 V at 0.05 mA cm^{-2} prior to each discharge.

Reference for Electronic Supplementary Information

(S1) X. Ren, S. Chen, H. Lee, D. Mei, M. H. Engelhard, S. D. Burton, W. Zhao, J. Zheng, Q. Li, M. S. Ding, M. Schroeder, J. Alvarado, K. Xu, Y. S. Meng, J. Liu, J. G. Zhang and W. Xu, *Chem*, **2018**, *4*, 1877–1892.